S.M. Frolov, S.N. Medvedev, V.Ya. Basevich, F.S. Frolov
Semenov Institute of Chemical Physics, Moscow, Russia

Self-ignition of hydrocarbon–hydrogen–air mixtures

Abstract. The objective of this work is the theoretical study of the effect of hydrogen admixing on self-ignition of homogeneous and hybrid (containing liquid drops) mixtures of heavy hydrocarbons (n-heptane and n-decane) in air based on the well-validated detailed reaction mechanism of n-decane oxidation. The self-ignition of homogeneous mixtures was studied using the kinetic code KINET, whereas the self-ignition of hybrid mixtures containing hydrocarbon drops, gaseous hydrogen and air was studied using DROP code, both developed at Semenov Institute of Chemical Physics. It has been shown that the reactivity of hydrogen-containing mixtures is not always higher than that of the pure hydrocarbon–air mixture. At temperatures less than approximately 1050 K, addition of hydrogen to hydrocarbon–air mixture was shown to increase the overall self-ignition delay, i.e. hydrogen plays the role of self-ignition inhibitor. In these conditions, with the increase of hydrogen content in homogeneous and hybrid mixtures the duration of the blue-flame reaction stage was shown to become shorter and even to degenerate. This phenomenon is caused by reactions of molecular hydrogen with the intermediate products of hydrocarbon oxidation leading to the formation of less active species like HO_2 radical hindering chain branching processes. Nevertheless, at temperatures exceeding approximately 1050 K hydrogen addition was shown to decrease the overall self-ignition delay time thus indicating that hydrogen serves as self-ignition promoter. These finding have to be taken into account when discussing the perspectives of practical applications of fuels blended with hydrogen as well as related explosion safety issues.

1 INTRODUCTION

Hydrogen exhibits unique properties – low density (0.08 kg/m^3 at 300 K and 1 atm), wide flammability limits (from 4%(vol.) to 75%(vol.) in air), high laminar flame velocity (2.3 m/s at normal conditions) and very low ignition energy (0.02 mJ). In addition, combustion of hydrogen–air mixtures is known to be accompanied with formation of only nitrogen oxides as pollutants and at fuel–air ratio $\Phi < 0.5$ their emissions nearly vanish. Therefore the idea of partial or complete replacement of hydrocarbon fuel with hydrogen in power plants and transportation engines is currently actively discussed in the literature [1]. However the relevant literature contains contradictory information on the effect of hydrogen.

For example, diesel engine performances under the operation on diesel oil blended with different secondary gaseous fuels were reported in [2]. Propane, methane, ethanol, and hydrogen were chosen as the secondary fuels. Self-ignition and combustion characteristics of blended fuels as well as emissions of NOx, CO and unreacted hydrocarbons were measured experimentally. The conclusion was made that using the knowledge of combustion characteristics of blended fuels to properly tune the operation process one can reduce considerably pollutant emissions, decrease the self-ignition delay and avoid engine knock.

In [3], experiments and numerical simulation of piston engine operation on n-heptane blended with hydrogen were performed to find out whether hydrogen addition decreases NOx emissions. As a matter of fact, hydrogen addition was shown to reduce NO emission but NO_2 emission appeared to be higher than that for the unblended fuel. Moreover, the ultimate emission of NOx also increased. Numerical simulations were unable to adequately predict the NOx emission level. To explain these findings, the author of [3] assumed that the increase of NO_2 concentration in the course of combustion of blended fuel is caused by higher concentrations of HO_2 radical serving as an oxidizing agent for NO. Note that hydrogen addition resulted in the reduction of emissions of soot, CO, CO_2, and unreacted hydrocarbons.

Despite self-ignition and combustion characteristics of hydrogen and many individual hydrocarbons are fairly well studied, there is not much data for hydrocarbon–hydrogen blends

1

related to their explosion safety. As a matter of fact, only limited data are available on blended fuel combustion (e.g., methane–hydrogen [4], propane–hydrogen [5], kerosene–hydrogen [6, 7]) and self-ignition (methane–hydrogen [8]). Surprisingly, the fact that hydrogen reactivity in air is not always higher than that of hydrocarbons, in particular at low temperatures, is not discussed at all in the relevant literature.

The objective of this paper is the theoretical study of the effect of hydrogen admixing on self-ignition of homogeneous and hybrid mixtures of heavy hydrocarbons (n-heptane and n-decane) in air based on the well-validated detailed reaction mechanism of n-decane oxidation.

2 CHEMICAL REACTION MECHANISM

For modeling the effect of hydrogen additives to homogeneous and hybrid (with liquid drops) mixtures of heavy hydrocarbons (n-heptane and n-decane) with air on self-ignition we used a well-validated, relatively compact detailed reaction mechanism of n-decane oxidation developed at Semenov Institute of Chemical Physics [9]. This mechanism contains only 1083 elementary processes that govern the reaction rate and the formation of basic intermediate and final products represented by 108 species. The mechanism has two essential features: (*i*) reactions of so called double addition of oxygen (first, to the alkyl radical, then to the isomerized form of the formed peroxide radical) are lacking because the first addition is considered to be sufficient; (*ii*) isomeric compounds and their derivative substances as intermediate species are not considered, because this means of oxidation is slower than through molecules and radicals of the normal structure. This mechanism was systematically validated for propane [10], n-butane [11], n-pentane [12], n-hexane [13], n-heptane [14], and n-decane [9]. The major feature of this mechanism is the appearance of stages, viz., cool and blue flames during low-temperature self-ignition.

To show the performance of the mechanism we present here some examples with the self-ignition of homogeneous mixtures using the kinetic code KINET developed at Semenov Institute of Chemical Physics. The code solves zero-dimensional time dependent equations of chemical kinetics coupled with the energy conservation equation for isobaric conditions.

Figure 1a presents typical calculated time dependences of temperature during the spontaneous ignition of a stoichiometric n-decane–air mixture, which are characteristic for low and high initial temperatures. The first stepped increase for the relatively low initial temperature $T_0 = 588$ K at $t \sim 1.27$ s is related to the appearance of the cool flame. The blue flame (clearly visible in Fig. 1b with a change of the scale) then appears after a lapse of about 0.28 s; the hot flame then appears at approximately 1.57 s and the temperature increases to 2500 K and higher. The stages of spontaneous ignition, i.e. stepwise appearance of cool, blue, and hot flames, occur as follows. The acceleration of the reaction in the cool flame is the consequence of branching during decomposition of alkyl hydroperoxide (here, alkyl hydroperoxide $C_{10}H_{21}O_2H$) with the formation of hydroxyl and oxyradical. The appearance of the blue flame is the consequence of branching because of the decomposition of hydrogen peroxide H_2O_2. This is clearly evident in Fig. 1b from the calculated kinetic curves for peroxide and the two peaks in the concentration of hydroxyl. The stages result in the phenomenon of the negative temperature coefficient (NTC) of the reaction rate; the overall self-ignition delays at a higher initial temperature appear to be greater than at a low temperature. This effect is clearly seen in Fig. 1a. Note that in the calculations, the overall self-ignition delay time t_{ign} was determined as the time taken for the temperature growth rate to attain the value of 10^7 K/s (other possible definitions were proved to give very similar results for t_{ign}).

Figures 2a and 2b compare calculated (curves) and measured (points) overall self-ignition delays t_{ign} for various initial temperatures and pressures. In all cases, the homogeneous mixture composition is stoichiometric ($1.33\% C_{10}H_{22}$ – air). The points on the graphs correspond to the experimental data of [15] for pressures of 12 and 50 atm, experimental data of [16] for pressures of 13 and 80 atm, experimental data of [17] for a pressure of 1 atm (Fig. 2a), and experimental data of [18, 19] for pressures of 10 and 40 atm (Fig. 2b).
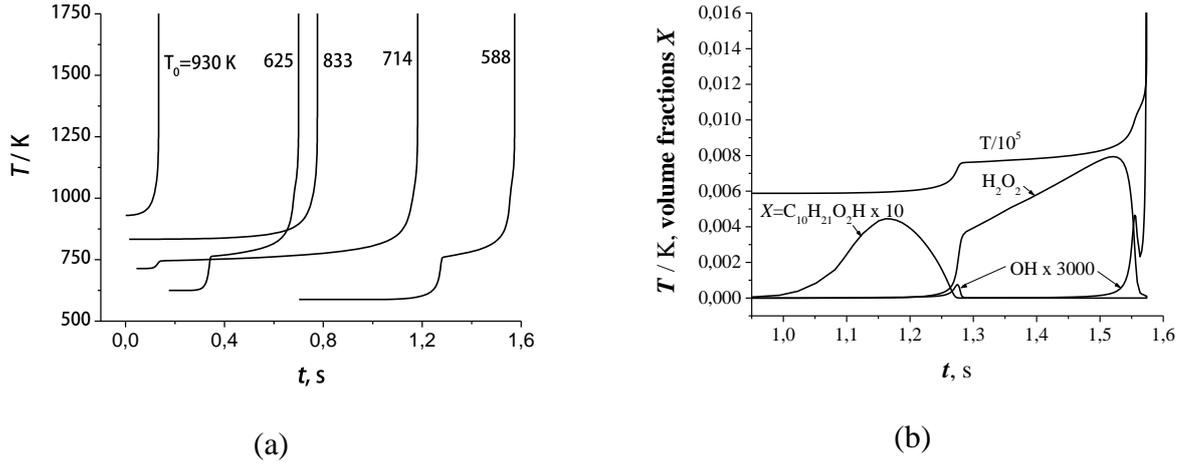
Figure 1: Calculations of spontaneous ignition of stoichiometric n-decane–air mixture at initial pressure $P_0 = 1$ atm: (a) time histories of temperature at $T_0 = 588, 625, 714, 833,$ and 930 K; (b) time histories of temperature and volume fractions of peroxides and hydroxyl at $T_0 = 588$ K.
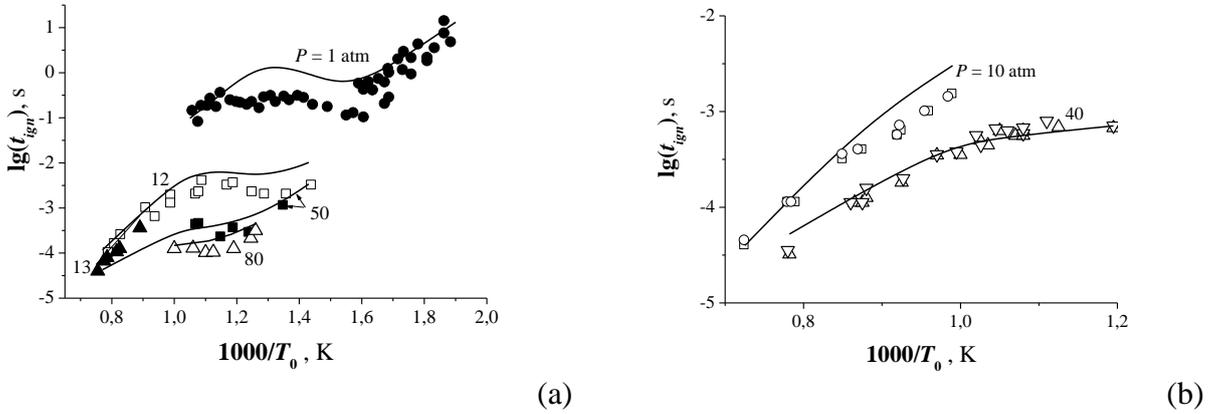

Figure 2: Comparison of measured (points) and calculated (curves) overall self-ignition delays of stoichiometric n-decane–air mixture at different temperatures and pressures: (a) experiments [15–17]; (b) experiments [18, 19].

It follows from Fig. 2 that the detailed reaction mechanism of n-decane oxidation provides satisfactory agreement with available experimental data on overall self-ignition delays in wide ranges of initial temperature and pressure. Note that hydrogen oxidation kinetics is included in the n-decane oxidation mechanism as a constituent part. Figure 3 demonstrates the performance of the hydrogen oxidation kinetics by means of comparison between calculated (curve) and measured (points) self-ignition delays for stoichiometric hydrogen − air mixture at different initial temperatures and pressure $P_0 = 1$ atm.

3 MODEL OF DROP SELF-IGNITION AND COMBUSTION

The liquid drop is assumed to be a sphere of radius r_s and occupy the region $0 < r < r_s$ at time t (index s relates to drop surface). The droplet size is allowed to vary in time due to thermal expansion and liquid vaporization processes. Therefore, r_s is treated as the moving boundary.

The continuity equation for liquid is

$$\frac{\partial \rho_d}{\partial t} + \frac{1}{r^2}\frac{\partial}{\partial r}\left(r^2 \rho_d u_d\right) = 0$$

where index d relates to liquid, r is the radial coordinate, ρ is the density, and u is the velocity.
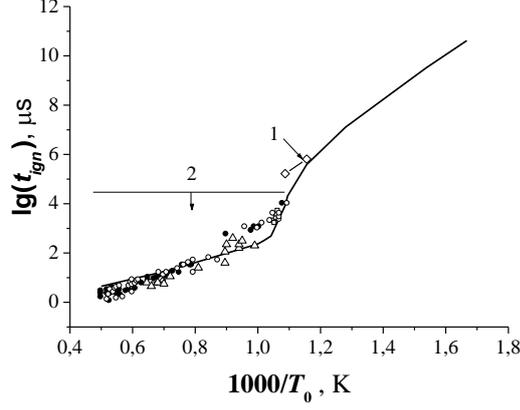
3

Figure 3: Comparison of measured (points) and calculated (curve) self-ignition delays of stoichiometric hydrogen–air mixture at different temperatures and $P_0 = 1$ atm: 1 − experiments cited in [20]; 2 − experiments [21].

Temperature distribution in liquid ($0 < r < r_s$), $T_d(r)$ is governed by the energy equation:

$$c_d \rho_d \frac{\partial T_d}{\partial t} + c_d \rho_d u_d \frac{\partial T_d}{\partial r} = \frac{1}{r^2} \frac{\partial}{\partial r}\left(\lambda_d r^2 \frac{\partial T_d}{\partial r}\right),$$

$$T_d(0,r) = T_{d0}, \quad \left.\frac{\partial T_d}{\partial r}\right|_{r=0} = 0, \quad T_d(t,r_s) = T_g(t,r_s),$$

where T is the temperature, c is the specific heat, and λ is the thermal conductivity.

The mass concentration of liquid vapor (index v) at the drop surface is

$$Y_v = \frac{P_v}{P}\frac{W_v}{\overline{W}},$$

where P is the pressure, W is the molecular mass, and bar denotes the mean value.

The gas phase (index g) is assumed to occupy region $r_s < r < R$, where R is the effective half-distance between drops in gas–drop suspension. This parameter can be found based on the simple formula

$$R = r_{s0}\left(\frac{\rho_d}{\eta}\right)^{1/3} = r_{s0}\left(\frac{\rho_d}{\rho_g \Phi \phi_{st}}\right)^{1/3}$$

where index 0 denots the initial value, η is the mass content of liquid in the unit volume of drop suspension, Φ is the fuel–air ratio, and ϕ_{st} is the stoichiometric fuel–air ratio ($\phi_{st} \approx 0.06$ for hydrocarbon fuels).

The gas flow around the drop is governed by the continuity equation

$$\frac{\partial \rho_g}{\partial t} + \frac{1}{r^2}\frac{\partial}{\partial r}(r^2 \rho_g u_g) = 0,$$

$$\left.\rho_d(u_d - \frac{\partial r_s}{\partial t})\right|_{r=r_s} = \left.\rho_g(u_g - \frac{\partial r_s}{\partial t})\right|_{r=r_s},$$

species continuity equation

$$\rho_g \frac{\partial Y_j}{\partial t} = \frac{1}{r^2}\frac{\partial}{\partial r}(\rho_g r^2 Y_j V_j) - \rho_g u_g \frac{\partial Y_g}{\partial r} + \omega_{gj}$$

$$Y_j(0,r) = Y_{j0} \quad j = 1, 2, ..., N,$$

$$\left.-\rho_d u_i \beta_j\right|_{r=r_s} = \left.\rho_g Y_j\left(u_g - \frac{\partial r_s}{\partial t}\right) + \rho_g Y_j V_j\right|_{r=r_s},$$

4

$$\left.\frac{\partial \overline{W} Y_j}{\partial r}\right|_{r=R} = 0, \quad j = 1,...,N$$

$$X_j = Y_j \overline{W} / W_j$$

$$\frac{\partial X_j}{\partial r} = \sum_{k=1}^{N}\left(\frac{X_j X_k}{D_{jk}}\right)(V_k - V_j)$$

$$\omega_{gj} = W_{gj} \sum_{k=1}^{L} (v''_{j,k} - v'_{j,k}) A_k T_g^{n_k} \exp\left(-\frac{E_k}{RT_g}\right) \prod_{l=1}^{N}\left(\frac{Y_{gl}\rho_g}{W_{gl}}\right)^{v'_{l,k}}$$

$$\beta_j = 1 \text{ at } j = v$$
$$\beta_j = 0 \text{ at } j \neq v$$

and energy equation

$$c_{pg}\rho_g \frac{\partial T_g}{\partial t} = \frac{1}{r^2}\frac{\partial}{\partial r}\left(\lambda_g r^2 \frac{\partial T_g}{\partial r}\right) - c_{pg}\rho_g u_g \frac{\partial T_g}{\partial r} + \Omega$$

$$T_g(0,r) = T_{g0}$$

$$T_g(t,r_s) = T_d(t,r_s), \quad \left.\frac{\partial T_g}{\partial r}\right|_{r=R} = 0$$

$$\Omega = \sum_{k=1}^{L} H_k A_k T_g^{n_k} \exp\left(-\frac{E_k}{RT_g}\right) \prod_{j=1}^{N}\left(\frac{Y_{gj}\rho_g}{G_{gj}}\right)^{v'_{j,k}},$$

where Y_j is the mass fraction of species j; D_j is the diffusion coefficient for species j; ω_j is the rate of variation of mass fraction of species j due to chemical reactions; Ω is the chemical heat source; A_k, n_k, E_k, and H_k are the preexponential factor, power exponent, activation energy, and heat effect of the kth reaction; N is the number of species; L is the number of reactions, respectively.

In addition to above equations, the boundary condition for tailoring temperature fields in liquid and gas at $r = r_s$

$$\lambda_d \frac{\partial T_d}{\partial r} - \frac{\rho_{ds} u_s L_v}{W_v} = \lambda_g \frac{\partial T_g}{\partial r},$$

equation of state for the gas phase

$$\rho_g = \frac{P\overline{W}}{R^o T_g},$$

and the condition of constant pressure

$$P = P_0 = const$$

are specified. Here, L_v is the latent heat of vaporization and R^o is the universal gas constant.

Molecular transport processes in liquid and gas phases as well as the corresponding specific heats are taken from [22].

To study ignition and combustion of hydrocarbon fuel drops in air, the detailed reaction mechanism of n-decane oxidation discussed in Section 2 was used.

The set of governing equations was integrated numerically using DROP code developed at Semenov Institute of Chemical Physics. Applied in the code is a nonconservative finite-difference scheme and adaptive moving grid. The computational error was continuously monitored by checking balances of C and H atoms as well as energy balance at each time step. More details on the computational procedure can be found in [23].
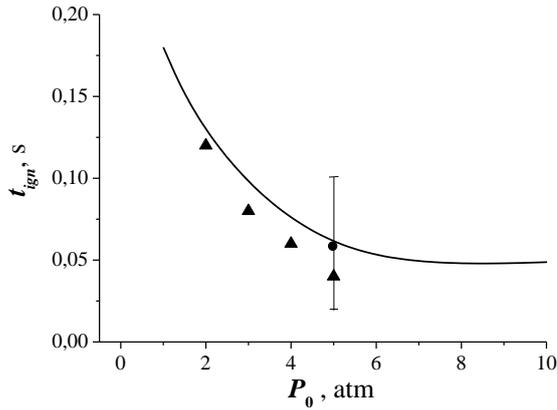
Figure 4: Calculated pressure dependence (curve) of self-ignition delay time t_{ign} for n-heptane drops with $d_0 = 700$ μm at $T_0 = 1000$ K against experimental data. Triangles – measured values of t_{ign} for single n-heptane drops with $d_0 = 700$–750 μm and $T_0 = 1000$ K [24]; circle – for drops with $d_0 = 700$ μm and $T_0 = 940$ K [25] (the vertical bar indicates the scatter in experimental data).
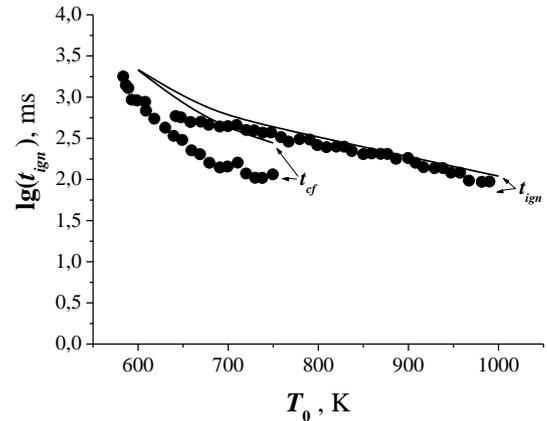
Figure 5: Comparison of calculated (curves) and measured (points [26]) dependences of the delay times of cool flame (t_{cf}) and hot flame (t_{ign}) appearance on the initial temperature for a single n-decane drop in air: $d_0 = 700$ μm, $P_0 = 1$ atm.

The model described above was validated against experimental data on drop self-ignition and combustion for various liquid hydrocarbons. As an example, Fig. 4 compares the calculated (curve) and measured (points [24, 25]) dependence of the overall ignition delay time t_{ign} for n-heptane drops. The definition of t_{ign} was the same as for the homogeneous mixtures but the criterion 10^7 K/s for the temperature growth rate was applied to the maximum gas temperature $T_{g,max}(t)$. As can be seen, the overall self-ignition delay time increases sharply at low pressures. Furthermore, Fig. 5 compares the calculated (curves) and measured (points from [26]) delay times of cool flame appearance (t_{cf}) and overall self-ignition delay time (t_{ign}) for n-decane drops of initial diameter 700 μm at different initial temperatures and pressure $P_0 = 1$ atm. The delay time of cool flame appearance (t_{cf}) was defined as the time taken for the maximum gas temperature $T_{g,max}$ to attain the inflection point at the first stepwise temperature variation in the $T_{g,max} - t$ plane. Clearly, the model predicts correctly not only qualitative features of drop self-ignition phenomenon but also provides satisfactory quantitative information. Note that cool flames during self-ignition of liquid sprays were observed experimentally long ago [27].

4 SELF-IGNITION OF HOMOGENEOUS HYDROCARBON–HYDROGEN–AIR MIXTURES

The reaction mechanism of Section 2 was first used to study the effect of hydrogen addition on the self-ignition delay time of homogeneous hydrocarbon–air mixtures. The calculations of mixture self-ignition and volumetric combustion were performed using KINET code.

Figure 6 shows the predicted dependences of overall self-ignition delays on temperature for homogeneous stoichiometric n-heptane–air mixtures with different content of hydrogen (from 0% (vol.) to 100% (vol.)) at pressure $P_0 = 15$ atm. At $T_0 \approx 1050$ K, the self-ignition delays of n-heptane–air and hydrogen–air mixtures are seen to be the same. At $T_0 < 1050$ K, addition of hydrogen to n-heptane–air mixture increases the self-ignition delay, whereas at $T_0 > 1050$ K – decreases it. Note that even in the mixtures with high amount of hydrogen (e.g., 90% (vol.)) the effect of NTC of reaction rate is clearly seen in Fig. 6.
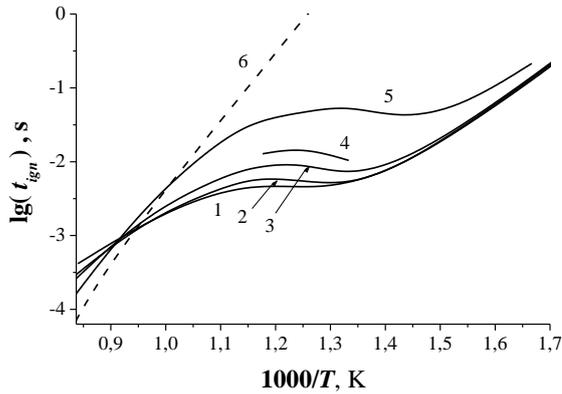
6

Figure 6: Predicted dependences of self-ignition delays on temperature for stoichiometric homogeneous C_7H_{16}–H_2–air mixtures with different hydrogen content: 1 – 0%(vol.), 2 – 10%, 3 – 50%, 4 – 70%, 5 – 90%, 6 – 100%; pressure $P_0 = 15$ atm.
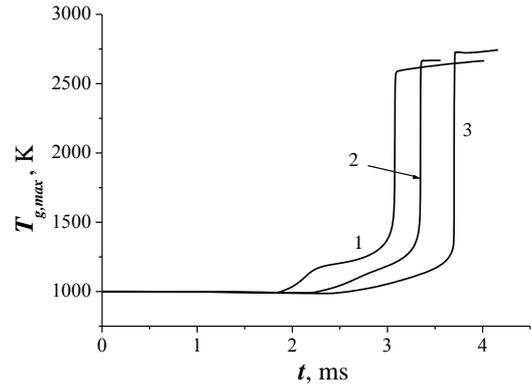
Figure 7: Predicted time histories of the maximum gas temperature $T_{g,max}$ in the stoichiometric mixture n-heptane (drops) – hydrogen – air at different initial hydrogen content: 1 – 0% (vol.), 2 – 7.5%(vol.) and 3 – 14.75% (vol.); $d_0 = 60$ μm, $P_0 = 20$ atm, $T_{g0} = 1000$ K.

5 SELF-IGNITION OF HYBRID HYDROCARBON (DROPS)–HYDROGEN–AIR MIXTURES

The reaction mechanism of Section 2 was then used to study the effect of hydrogen addition on the self-ignition delay time of hybrid hydrocarbon drops – hydrogen – air mixtures. The calculations of ignition and combustion of such mixtures were performed using DROP code.

Figure 7 shows the predicted time histories of the maximum gas temperature $T_{g,max}$ at self-ignition of hybrid stoichiometric compositions containing n-heptane drops, air, and hydrogen with different volumetric content: 0%, 7,5% and 14,75%. The calculations were made for drops of $d_0 = 60$ μm at $T_0 = 1000$ K and $P_0 = 20$ atm.

The stoichiometric composition of hybrid mixture was set according to the following procedure. First, the volume of air needed for complete oxidation of hydrocarbon fuel was determined. Then a certain amount of hydrogen was added to this volume of air. Finally, the resultant homogeneous hydrogen–air mixture was diluted with such an amount of additional air which was needed for complete oxidation of hydrogen. Based on this procedure, the volume fraction of hydrogen in the gas phase was determined.

The analysis of spatial distributions of intermediate reaction products indicates that the staged behavior of the maximum gas temperature $T_{g,max}$ in Fig. 7 is caused by the appearance of the blue flame due to decomposition of hydrogen peroxide accumulated in a local region in the close vicinity to the drop surface. With the increase of hydrogen content in the hybrid mixture, the duration of the blue-flame reaction stage becomes shorter and the overall self-ignition delay time increases. When taking Fig. 6 into account, this result could be treated as trivial because at $T_0 = 1000$ K the overall self-ignition delay in the homogeneous stoichiometric n-heptane – air mixture is approximately a factor of 2 shorter than that in the homogeneous stoichiometric hydrogen – air mixture. However one has to keep in mind that Fig. 7 relates to the self-ignition of hybrid rather than homogeneous mixture. At self-ignition of liquid drops the temperature and fuel vapor concentration in the vicinity of the drop surface are highly nonuniform. Moreover, self-ignition of fuel vapor occurs in the region where the gas temperature is lower than its value at a large distance from the drop surface and the fuel vapor – air mixture is essentially fuel lean [23]. In view of it, the results of Fig. 7 are not trivial. Note also that the degeneration of the blue flame stage of n-heptane oxidation is caused by reactions of molecular hydrogen with the inter-
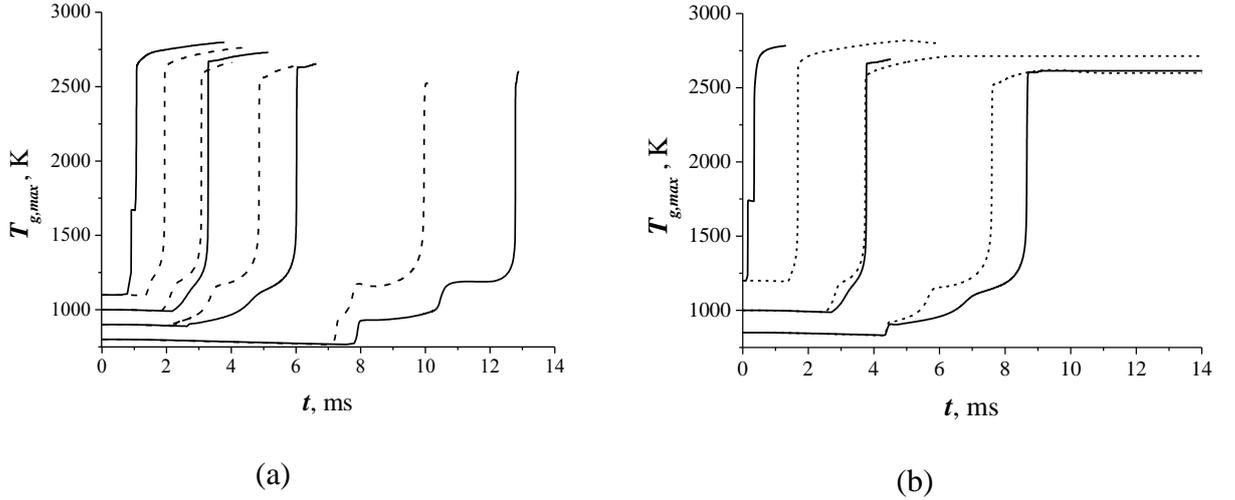
7

Figure 8: Predicted time histories of the maximum gas temperature $T_{g,max}$ in the stoichiometric mixtures n-heptane (drops)–hydrogen–air (a) and n-decane (drops)–hydrogen–air (b) at different initial temperatures and different initial hydrogen content: 7.5%(vol.) H_2 (solid curves) and 0% H_2 (dashed curves); drop diameter $d_0 = 60$ μm, $P_0 = 20$ atm.

medient products of fuel oxidation, in particular with alkyl hydroperoxides, hydrogen peroxide and products of their decomposition leading to the formation of less active radicals like HO_2.

These considerations are confirmed by the results of calculations presented in Fig. 8. Shown in Fig. 8 are the predicted time histories of maximum gas temperature at self-ignition of n-heptane (Fig. 8a) and n-decane (Fig. 8b) drop suspensions in air mixed with 7.5%(vol.) hydrogen (solid curves) and in pure air (dashed curves) at $P_0 = 20$ atm and different initial temperatures. It is clearly seen that hydrogen addition affects not only the overall self-ignition delay time t_{ign} but also the duration of intermediate stages of multistage self-ignition (cool and blue flames). At a relatively low temperature (e.g., at $T_0 = 800$ K) the duration of cool and blue flame stages increases considerably. This indicates that molecular hydrogen deactivates active intermediate radicals participating in the channels of chain origination, propagation, and branching. Nevertheless, similar to homogeneous mixtures, at $T_0 < 1050$ K the self-ignition delay time in the hydrogen-containing hybrid mixtures increases as compared to the mixtures without hydrogen, whereas at $T_0 > 1050$ K it decreases.

The detailed analysis of various physical and chemical processes in the vicinity to the drop surface reveals several more interesting features of hybrid mixture self-ignition. For example, Fig. 9 shows the time histories of the normalized mass content of fuel vapor I_v (Fig. 9a) and hydrogen peroxide $I_{H_2O_2}$ (Fig. 9b) in the sphere of radius R around the fuel drop in uniform stoichiometric n-heptane drop suspension (R is the effective half-distance between drops in gas–drop suspension, see Section 3). The normalized mass content of the ith species in the gas phase is defined as:

$$I_i(t) = m_0^{-1} \int_{r_s(t)}^{R} 4\pi\xi^2 Y_i(\xi,t)d\xi$$

where m_0 is the initial mass of the fuel drop.

The overall self-ignition delay time in Fig. 9 associated with a sharp depletion of fuel vapor and hydrogen peroxide is seen to increase with hydrogen content. Also, addition of increasing amounts of hydrogen to the gas–drop suspension results in faster drop vaporization (caused by high hydrogen specific heat and diffusivity) and larger amounts of fuel vapor and hydrogen peroxide accumulated near the drop before self-ignition occurs. As was mentioned above, such a behavior of the overall self-ignition delay time is caused by reactions of molecular
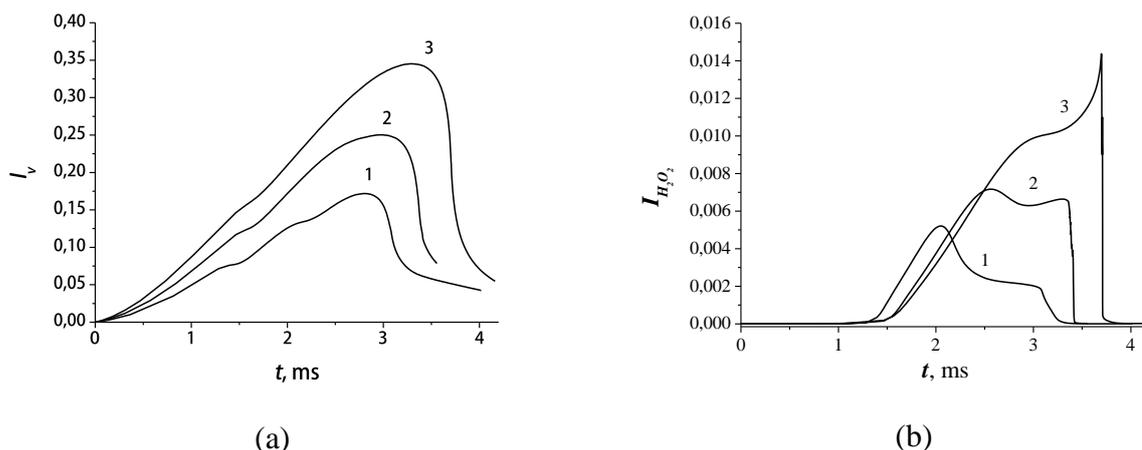
8

Figure 9: Predicted time histories of the normalized mass contents of fuel vapor (a) and hydrogen peroxide (b) around a drop in uniform stoichiometric n-heptane drop suspension at different initial volumetric H_2 content: 1–0%, 2–7.5%, and 3–14.5%; $d_0 = 60$ μm, $P_0 = 20$ atm.

hydrogen with the intermediate products of n-heptane oxidation leading to the formation of less active radicals like HO_2.

CONCLUSIONS

The detailed reaction mechanism of n-decane oxidation in air was used to simulate self-ignition of stoichiometric homogeneous hydrocarbon–hydrogen–air mixtures and hybrid mixtures of hydrocarbon drops with hydrogen and air at different initial temperature, pressure and volumetric hydrogen content (from 0% to 14.7%). Two hydrocarbons were investigated: n-heptane and n-decane.

It has been shown that the reactivity of hydrogen-containing mixtures is not always higher than that of the pure hydrocarbon–air mixture. At approximately $T_0 < 1050$ K, addition of hydrogen to hydrocarbon–air mixture was shown to increase the overall self-ignition delay time, i.e. hydrogen plays the role of self-ignition inhibitor. In these conditions, with the increase of hydrogen content in homogeneous and hybrid mixtures the duration of the blue-flame reaction stage was shown to become shorter and even to degenerate. This phenomenon is caused by reactions of molecular hydrogen with the intermediate products of hydrocarbon oxidation leading to the formation of less active species like HO_2 radical hindering chain branching processes. Nevertheless, at approximately $T_0 > 1050$ K hydrogen addition was shown to decrease the overall self-ignition delay time thus indicating that hydrogen serves as self-ignition promoter. These findings have to be taken into account when discussing the perspectives of practical applications of fuels blended with hydrogen and relevant explosion safety issues.

ACKNOWLEDGEMENTS

REFERENCES

1. Verhelst S., Wallner T. Hydrogen-fueled internal combustion engines. Progress in Energy and Combustion Science, 2009, Vol. 35, P. 490–527.
2. Karim G.A. Combustion in gas fueled compression: ignition engines of the dual fuel type. Journal of gas turbine and power, 2003, Vol. 215, P. 827.
3. McWilliam L. Combined hydrogen diesel combustion: an experimental investigation into the effects of hydrogen addition on the exhaust gas emissions, particulate matter size distribution and chemical composition. Ph.D. thesis, 2008, P. 1.
4. Zhanga Y., Wu J., Ishizuka S. Hydrogen addition effect on laminar burning velocity, flame temperature and flame stability of a planar and a curved CH_4–H_2–air premixed flame. Int. J. Hydrogen Energy, 2009, Vol. 34, P. 519–527.
5. Cheng R.K., Littlejohn D., Strakey P.A., Sidwell T. Laboratory investigations of a low-swirl injector with H_2 and CH_4 at gas turbine conditions. Proc. Combust. Inst., 2009, Vol. 32(II), P. 3001–3009.
6. Burguburu J., Cabot G., Renou B., Boukhalfa A.M., Cazalens M. Effects of H_2 enrichment on flame stability and pollutant emissions for a kerosene/air swirled flame with an aeronautical fuel injector. Proc. Comb. Inst., 2011, Vol. 33, P. 2927–2935.
7. Frenillota J.P., Cabota G., Cazalens M., Renoua B., Boukhalfa M.A. Impact of H_2 addition on flame stability and pollutant emissions for an atmospheric kerosene/air swirled flame of laboratory scaled gas turbine. Int. J. Hydrogen Energy, 2009, Vol. 34, P. 3930–3944.
8. Cheng R.K., Oppenheim A.K. Autoignition in methane-hydrogen mixtures. Combustion and flame, 1984, Vol.58, P. 125-139.
9. Basevich V. Ya., Belyaev A. A., Medvedev S. N., Posvyanskii V. S., and Frolov S. M. Oxidation and Combustion Mechanisms of Paraffin Hydrocarbons: Transfer from C_1–C_7 to C_8H_{18}, C_9H_{20}, and $C_{10}H_{22}$. Russian Journal of Physical Chemistry B, 2011, Vol. 5(6), P. 974–990.
10. Basevich V. Ya., Belyaev A. A., and Frolov S. M., The mechanisms of oxidation and combustion of normal alkane hydrocarbons: The transition from C_1–C_3 to C_4H_{10}// Russian Journal of Physical Chemistry B, 2007, Vol. 2(5), P. 477–484.
11. Basevich V. Ya., Vedeneev V. I., Frolov S. M., and Romanovich L. B. Nonextensive principle to construct oxidation and combustion mechanisms of normal alkane hydrocarbons: The transition from C_1–C_2 to C_3H_8. Rus. J. Chem. Phys., 2006, 25 (11), P. 87.
12. Basevich V. Ya., Belyaev A. A., and Frolov S. M. Mechanisms of the oxidation and combustion of normal alkanes: The transition from C_1-C_4 to C_5H_{12}. Russ. J. Phys. Chem. B, 2009, Vol. 3, P. 629.
13. Basevich V. Ya., Belyaev A. A., and Frolov S. M. Mechanisms of the oxidation and combustion of normal alkanes: Transition from C_1–C_5 to C_6H_{14}. Russ. J. Phys. Chem. B, 2010, Vol. 4, P. 634.
14. Basevich V. Ya., Belyaev A. A., Posvyanskii V. S., and Frolov S. M. Mechanism of the oxidation and combustion of normal paraffin hydrocarbons: Transition from C_1–C_6 to C_7H_{16}. Russ. J. Phys. Chem. B, 2010, Vol. 4, P. 985.
15. Pfahl U., Fieweger K., Adomeit G. Self-ignition of diesel-relevant hydrocarbon-air mixtures under engine conditions. Proc. 26th Symp. (Int.) on Comb. Comb. Inst., Pittsburgh, 1996, P. 781.
16. Zhukov V.P., Sechenov V.A., Starikovskii A.Yu. Autoignition of n-decane at high pressure. Comb. Flame, 2008, V.153, P.130.
17. Troshin K.Ya. Experimental study of the ignition of n-hexane- and n-decane-based surrogate fuels. Russ. J. Chem. Phys. 2008, Vol. 2(3), P. 419-425.

18. Shen H.-P.S., Steinberg J., Vanderover J. et al. A shock tube study of the ignition of n-heptane, n-decane, n-dodecane, and n-tetradecane at elevated pressures. Energy Fuels. 2009, V. 23, P. 2482.
19. Wang H., Warner S.J., Oehlschlaeger A. et al. An experimental and kinetic modeling study of the autoignition of α-methylnaphthalene/air and α-methylnaphthalene/n-decane/air mixtures at elevated pressures. Comb. Flame, 2010, Vol.157, P. 1976-1988.
20. Anagnostou E., Brokaw R. S. and Butler J. N. Effect of concentration on ignition delays for various fuel-oxygen-nitrogen mixtures at elevated temperatures. NACA TN 3887, 1956.
21. Golovichev V.I. Numerical integration of chemical-kinetics equations. Combustion, Explosion, and Shock Waves, 1973, Vol.9(4), P. 418.
22. Reid R. C., Prausnitz J. M., Sherwood T. K. The Properties of Gases and Liquids. N.Y., McGrow–Hill, 1977.
23. Frolov S.M., Basevich V.Ya., Frolov F.S., Borisov A.A., Smetanyuk V.A., Avdeev K.A., Gotz A.N. Correlation between drop vaporization and self-ignition. Rus. J. Chem. Physics, 2009, Vol. 28(5), P.3–18.
24. Tanabe M., Bolik T., Eigenbrod C., and Rath H. J. Spontaneous ignition of liquid droplets from a view of non-homogeneous mixture formation and transient chemical reactions. Proc. Combust. Inst., 1996, Vol. 26, P. 1637-1643.
25. Schnaubelt S., Moriue O., Coordes T., Eigenbrod C., and Rath H. J. Detailed numerical simulations of the multistage self-ignition process of n-heptane, isolated droplets and their verification by comparison with microgravity experiments. Proc. Combust. Inst., 2000, Vol. 28, P. 953.
26. Moriue O., Eigenbrod C., Rath H. J., et al., Effects of dilution by aromatic hydrocarbons on staged ignition behavior of n-decane droplets. Proc. Combust. Inst., 2000, Vol. 28, P. 969.
27. Sokolik A. S. and Basevich V. Ya. On the kinetic nature of self-ignition in diesel engine conditions. Sov. J. Phys. Chem., 1954, Vol. 28, P. 1935.